# Maximum a posteriori multiple source localization with Gibbs Sampling

**Zoi-Heleni Michalopoulou**

Department of Mathematical Sciences
New Jersey Institute of Technology
Newark, NJ 07102

CAMS Report 0506-22, Spring 2006

Center for Applied Mathematics and Statistics

NJIT

**Abstract**

Multiple source localization in underwater environments is approached within a matched-field processing framework. A Maximum a Posteriori Estimation method is proposed that estimates source location and spectral characteristics of multiple sources via Gibbs Sampling. The method facilitates localization of weak sources which are typically masked by the presence of strong interferers. A performance evaluation study based on Monte Carlo simulations shows that the proposed Maximum a Posteriori Estimation approach is superior to simple coherent matched-field interference cancellation. The proposed method is also tested on the estimation of the number of sources present, providing probability distributions in addition to point estimates for the number of sources.

# I Introduction

Acoustic source localization in shallow water environments is a challenging task hampered by the effects of sound interactions with the inadequately understood propagation medium. Loud interfering sources often present in coastal waters mask the source of interest, further complicating localization.

Matched field processing (MFP) [1, 2] has been extensively used for source localization in the ocean. The measured acoustic data are compared to field replicas generated with a sound propagation model and estimates are taken to be those parameter values that generate the best match between true and replica fields according to some specified matching criterion.

Variants of MFP have been proposed for localization of multiple sources. Model-based methods in underwater environments were discussed in [3, 4, 5, 6, 7]; these multiple source localization techniques typically rely on eigenvector decompositions, modified Bartlett functions, or combination of these two approaches. The CLEAN method, widely used in astronomy for denoising images, was proposed in [1] for weak source localization by cancelling strong interferers. In this paper we propose a new processor that estimates multiple source locations with a Maximum a Posteriori approach optimized with Gibbs Sampling. The pro-

cessor forms joint posterior probability distributions of locations of multiple sources, source spectra, noise variance, as well as number of sources that are present. It is compared and found superior to simple coherent interference cancellation for multiple source localization through a Monte Carlo performance evaluation. Our method not only produces point estimates of the unknown parameters but probability distributions as well, capturing uncertainty in the estimation problem. With sampling performed from conditional posterior probability distributions, the method searches the parameter space efficiently, concentrating on regions that generate significant probability.

The structure of the paper is as follows: Section II discusses the CLEAN inteference approach as described for conventional MFP multiple source localization. Section III describes the new processor, deriving conditional posterior distributions that are necessary for the operation of the Gibbs Sampler. Section IV compares the proposed processor to a simple coherent CLEAN processor, relying on Bartlett ambiguity surfaces and subtraction of strong field components, through a performance evaluation with synthetic data. Estimation of the number of sources is discussed in Section V. Section VI summarizes the work and presents conclusions.

# II Matched-field processing and interference cancellation

In [1] it was suggested that the CLEAN deconvolution technique [8, 9], widely used since the late seventies for image enhancement especially in astronomy, might be a suitable tool in localization using MFP in the presence of multiple sources. Estimates of contributions from strong interferers are subtracted from the field received at a set of sensors in an effort to reveal weaker sources of interest which are otherwise masked. Proper subtraction of field components from received signals requires accurate knowledge of how signals propagate from

source to receiver. Essentially, we need to subtract from the sensed data the convolution of the source waveform and the medium impulse response, deconvolving interference from the received field.

It was proposed in [1] that, assuming a perfectly known environment, an ambiguity surface $P(r, z_s)$ (Bartlett, for example) is first constructed:

$$P(r, z_s) = \frac{\mathbf{G}(r, z_s)^* \mathbf{X}\mathbf{X}^* \mathbf{G}(r, z_s)}{||\mathbf{G}(r, z_s)||^2}, \tag{1}$$

where $\mathbf{G}(r, z_s)$ is a Green's function vector calculated for source range $r$ and depth $z_s$, and $\mathbf{X}$ is a vector containing received data. Specifically, assuming a strong and a weak source being present:

$$\mathbf{X} = \alpha_{str}\mathbf{G}(r_{str}, z_{s,str}) + \alpha_w \mathbf{G}(r_w, z_{s,w}) + \mathbf{W}, \tag{2}$$

where $\alpha_{str}$ and $\alpha_w$ are the complex amplitudes of the two source signals, $r_{str}$ and $r_w$ are the ranges for the strong and weak source and $z_{s,str}$ and $z_{s,w}$ are the corresponding depths, $\mathbf{G}(r_{str}, z_{s,str})$ and $\mathbf{G}(r_w, z_{s,w})$ are Green's function vectors calculated at the $L$ receiving phones for the strong and weak source, respectively, and $\mathbf{W}$ is an $L$-dimensional complex, zero-mean noise vector.

The maximum of this ambiguity surface is expected to lead to the source location estimates $\hat{r}_{str}$ and $\hat{z}_{s,str}$, of the strongest source present. Subsequently, a new surface $P_{str}$ is produced, using now as data the replica field computed at the estimated source location of the previous step:

$$P_{str}(r, z_s) = \frac{\mathbf{G}(r, z_s)^* \hat{\mathbf{G}}_{str} \hat{\mathbf{G}}_{str}^* \mathbf{G}(r, z_s)}{||\mathbf{G}(r, z_s)||^2}, \tag{3}$$

where $\hat{\mathbf{G}}_{str} = \mathbf{G}(\hat{r}_{str}, \hat{z}_{s,str})$.

This new ambiguity surface is subtracted from the original surface; the residual ambiguity surface $P_{res}(r, z_s)$is scanned again for a new source location. The subtraction is repeated until $M$ sources are identified, where $M$ is the number of sources believed to be present.

This "cleaning" approach cancels contributions of strong sources-interferers in an incoherent manner, because the subtraction is performed at the ambiguity surface level. In essence, we calculate $P_{res}(r, z_s)$ as follows:

$$P_{res}(r, z_s) = P(r, z_s) - k\ P_{str}(r, z_s), \tag{4}$$

where $k$ is a factor depending on the strength of the loud source.

In our work, we decided to use in place of $k$ an estimate of the strength of the loud source $|\hat{\alpha}_{str}|^2$. Optimally, a maximum likelihood estimate $\hat{\alpha}_{str}$ of $\alpha_{str}$ under the assumption that the data are embedded in Gaussian, spatially white noise can be obtained as follows:

$$\hat{\alpha}_{str} = \frac{\hat{\mathbf{G}}^*_{str}(\mathbf{X} - \alpha_w \mathbf{G}_w)}{||\hat{\mathbf{G}}_{str}||^2}, \tag{5}$$

where $\mathbf{G}_w = \mathbf{G}(r_w, z_{s,w})$.

Estimation using Equation 5 presumes knowledge of $\alpha_w$ and $\mathbf{G}_w$ which is not available. If, however, the strength of the weak source is much smaller than that of the strong source, that is, $|\alpha_w| << |\alpha_{str}|$, $\mathbf{X} \approx \alpha_{str}\mathbf{G}_{str} + \mathbf{W}$ and

$$\hat{\alpha}_{str} \approx \frac{\hat{\mathbf{G}}^*_{str}\mathbf{X}}{||\hat{\mathbf{G}}_{str}||^2}. \tag{6}$$

Equation 4 now becomes:

$$P_{res}(r, z_s) = P(r, z_s) - |\hat{\alpha}_{str}|^2\ P_{str}(r, z_s), \tag{7}$$

The process of Equation 7 removes from the original ambiguity surface $P(r, z_s)$ some of the contributions of the strong source (provided that the estimate for the strong source power is reasonable); other contributions (namely, $\mathbf{G}^*\alpha_w\mathbf{G}_w\alpha^*_{str}\mathbf{G}^*_{str}\mathbf{G}/||\mathbf{G}||^2$ and $\mathbf{G}^*\alpha_{str}\mathbf{G}_{str}\alpha^*_w\mathbf{G}^*_w\mathbf{G}/||\mathbf{G}||^2$) are not subtracted. In an attempt to remove as comprehensively as possible the strong source contributions, we propose a coherent application of the previously described CLEAN approach that removes the strong source components at the field

rather than the ambiguity surface level. A simple coherent CLEAN process is implemented as follows. Estimates of the source location $\hat{r}_{str}$ and $\hat{z}_{s,str}$ and replica $\mathbf{G}(\hat{r}_{str}, \hat{z}_{s,str})$ are obtained in the way already described. Estimate $\hat{\alpha}_{str}$ is then calculated from Equation 6. A new ambiguity surface, $P_{res,coh}(r_w, z_{s,w})$, is calculated as follows:

$$P_{res,coh}(r, z_s) = \frac{\mathbf{G}(r, z_s)^* \mathbf{Y}\mathbf{Y}^* \mathbf{G}(r, z_s)}{||\mathbf{G}(r, z_s)||^2}, \tag{8}$$

where $\mathbf{Y} = \mathbf{X} - \hat{\alpha}_{str}\mathbf{G}(\hat{r}_{str}, \hat{z}_{str})$. Assuming that two sources, a strong and a weaker one, are present, the ambiguity surface of Equation 8 corresponds to the contribution of the weak source field, and its maximization is expected to provide the location of the weak source. Again, the success of this method in estimating the location the weak source depends on the quality of $\mathbf{G}(\hat{r}_{str}, \hat{z}_{s,str})$ and $\hat{\alpha}_{str}$.

# III Localization of multiple sources with Maximum a Posteriori Estimation and Gibbs sampling

In [10] a Gibbs Sampling scheme was presented developing an estimate of the joint posterior distribution $p(r, z_s, \alpha, \sigma^2|\mathbf{X})$, where $r$ and $z_s$ are the source range and depth respectively, $\alpha$ is the complex spectrum of the source, $\sigma^2$ is the variance of additive Gaussian noise, and $\mathbf{X}$ is the observed data at a set of $L$ spatially (vertically here) separated hydrophones. From this joint distribution, the marginal posterior distribution $p(r, z_s|\mathbf{X})$ for source range and depth is calculated, maximization of which leads to maximum a posteriori estimates for source location [10, 11]. The estimate of the joint posterior distribution was derived using a Gibbs Sampler [12, 13, 14, 15, 16, 10] that draws samples in a cyclical fashion from marginal conditional posterior distributions.

The signal model in the frequency domain considered for the single source problem of [10]

is as follows:

$$\mathbf{X} = \alpha\mathbf{G} + \mathbf{W}, \tag{9}$$

where $\mathbf{G}$ is a Green's function vector calculated at the $L$ receiving phones, $\alpha$ is a complex factor containing source amplitude and phase, and $\mathbf{W}$ is an L-dimensional vector, each sample of which is drawn from a complex normal zero mean distribution with variance $2\sigma^2$.

The approach of [10] was developed for a simple source; the technique is extended in this paper for $M$ sources, $M \geq 1$. The signal model then becomes:

$$\mathbf{X} = \sum_{i=1}^{M} \alpha_i \mathbf{G}_i + \mathbf{W}. \tag{10}$$

Here, $\mathbf{G}_i = \mathbf{G}(r_i, z_{si})$, $r_i$ and $z_{si}$ are the range and depth of the $i$th source, $\alpha_i$ are complex factors containing amplitude and phase information for the i$th$ source. The number of sources $M$ is assumed known.

Using the same prior distributions as in [10], the joint posterior distribution of all parameters is as follows:

$$p(r_1, z_{s1}, \ldots, r_M, z_{sM}, \alpha_1, \ldots, \alpha_M, \sigma^2|\mathbf{X}))] \propto \frac{1}{(2\pi)^L} \frac{1}{\sigma^{2L+2}} \exp(-\frac{1}{2\sigma^2}||\mathbf{X} - \sum_{i=1}^{M} \alpha_i \mathbf{G}_i(r_i, z_{si})||^2). \tag{11}$$

For the marginal posterior distribution of $\alpha_i$ we need to fix $r_j$, $z_{sj}$, $j = 1, \ldots, M$, $\alpha_j$, $j, = 1, \ldots, M$, $j \neq i$, and $\sigma^2$ in Equation 11. The marginal posterior distribution of $\alpha_i$ conditional on all other unknowns can be rewritten as:

$$\begin{aligned} p(\alpha_i|r_1, z_{s1}, \ldots, r_M, z_{sM}, \alpha_j(j = 1, \ldots, M; j \neq i)), \sigma^2, \mathbf{X}) \quad = \\ M_{\alpha i} \exp(-\frac{||\mathbf{G}_i||^2}{2\sigma^2}||(\alpha_i - (\mathbf{G}_i^*(\mathbf{X} - \sum_{j=1,\ldots,M; j\neq i} \alpha_j \mathbf{G}_j))/||\mathbf{G}_i||^2)||^2) \end{aligned} \tag{12}$$

where $M_{\alpha_i}$ is a constant with respect to $\alpha_i$. Complex variable $\alpha_i$ is, thus, normally distributed with mean $(\mathbf{G}_i^*(\mathbf{X} - \sum_{j=1,\ldots,M; j\neq i} \alpha_j \mathbf{G}_j))/||\mathbf{G}_i||^2$ and variance $2\sigma^2/||\mathbf{G}_i||^2$.

The conditional posterior distribution for the variance is identified as an inverse $\chi^2$ distribution:

$$p(\sigma^2|r_1, z_{s1}, \ldots, r_M, z_{sM}, \alpha_1, \ldots, \alpha_M, \mathbf{X})) = \frac{1}{\sigma^{2L+2}} \exp(-\frac{1}{2\sigma^2}||\mathbf{X} - \sum_{i=1}^{M} \alpha_i \mathbf{G}_i(r, z_s)||^2). \quad (13)$$

Samples from both the normal and $\chi^2$ distributions can be readily generated [17].

The conditional distribution of $r_i$ and $z_{si}$ is as follows:

$$p(r_i, z_{si}|r_j, z_{sj}(j = 1, \ldots, M; j \neq i), \alpha_i(i = 1, \ldots, M), \sigma^2, \mathbf{X})) = K \exp(-\frac{1}{2\sigma^2}||\mathbf{X} - \sum_{j=1}^{M} \alpha_j \mathbf{G}_j(r_j, z_{sj})||^2), \quad (14)$$

where $K$ is a constant. In the distribution of Equation 14, $r_j$ and $z_{sj}$ for all $j$ are fixed with the exception of $r_i$ and $z_{si}$, $i \neq j$. The distribution of Equation 14 is evaluated on a grid for $r_i$ and $z_{si}$ similarly to the implementation in Ref. [18] and following the griddy Gibbs modeling of Ref. [19], because no closed form is known.

Gibbs sampling begins with a set of randomly chosen initial conditions for all unknown parameters ($r_i$, $z_{si}$, $\alpha_i$, and $\sigma^2$, $i = 1, \ldots, M$). The process as implemented here first draws a sample from the conditional distribution of range $r_1$ and source depth $z_{s1}$; this two-dimensional sample contains the new, updated values of range and depth for the first source and first iteration. Subsequently, a sample is drawn from the Gaussian marginal conditional posterior of $\alpha_1$ (Equation 12). The same process is repeated for $r_j$, $z_{sj}$, $\alpha_j$, $j = 2, \ldots, M$. Lastly, a sample is drawn for the variance from the inverse $\chi^2$ distribution of Equation 13, completing the first iteration. For a large number of iterations, the obtained sample sequences eventually converge to the true joint posterior distribution of $r_i$, $z_{si}$, $\alpha_i$, $i = 1, \ldots, M$, and $\sigma^2$ [15, 12, 13].

# IV Performance evaluation of the MAP processor

To evaluate the proposed method, we generated synthetic data simulating sound propagating in a shallow water environment. Received field data at a vertical array of 24 phones were generated corresponding to two sound sources. A strong source was at a range and depth of 4 km and 2 m, respectively. A weaker source was at a range and depth of 2.4 km and 48 m. The complex amplitudes of the strong source and weak source were $\alpha_1 = \alpha_{str} = 20\exp(i/2)$ and $\alpha_2 = \alpha_w = 2\exp(3i/2)$.

SNR varied between 7 and 24 dB. For the performance evaluation we generated 100 noisy realizations per case. We then performed source localization with a simple incoherent cancellation Bartlett processor (Equation 7), a simple coherent cancellation Bartlett processor (Equation 8), and the MAP estimator proposed here, and, for each method, estimated probabilities of correct localization. Correct localization is here defined as obtaining estimates between 2.22 and 2.58 km for range and between 42 and 54 m for depth for the weak source and between 3.82 and 4.18 km for range and 0 and 8 m for depth for the strong source. The search interval for range was between 0 and 5 km with a 2 m spacing; the interval for depth was between 0 and 72 m with a 2 m spacing. The Gibbs sampler was run for 2000 iterations, the first 200 of which were discarded. Initial values used in the Gibbs Sampler were 10 for $\sigma^2$, 100 for complex amplitudes of both sources, 2 km and 18 m for range and depth for the weak source and 3 km and 18 m for range and depth for the strong source. Experimentation was performed with higher iteration numbers and different initial conditions without significant changes in the results.

Figure 1 shows probability of correct localization for the coherent cancellation Bartlett processor and the MAP processor, where both sources transmit at 600 Hz; probability of correct localization as obtained for the incoherent cancellation Bartlett processor varied

between 0 and 0.06 and is not included in the figure. The two processors perform similarly, with the simple processor being slightly better at high SNRs and the coherent CLEAN processor optimized via Gibbs Sampling being minimally superior at lower SNRs.

Figure 2 shows probability of correct localization vs. SNR for the simple coherent Bartlett canceler and the MAP processor for a frequency of 200 Hz; in this case as well, the incoherent canceler provided low probability of correct localization and is not included in the figure. The performance of the MAP processor dominates that of the coherent Bartlett processor for the entire SNR range.

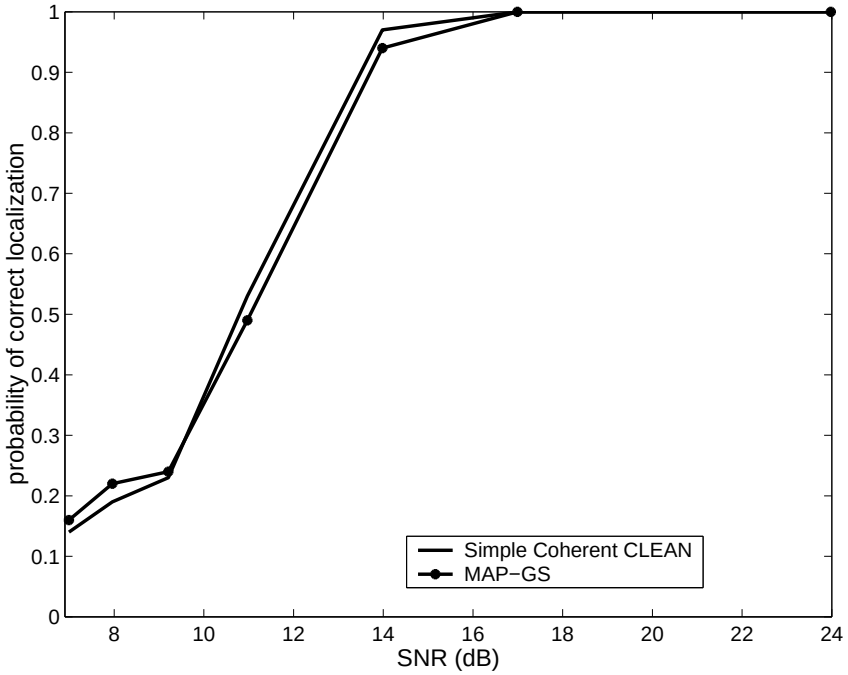


Figure 1: Probability of correct localization vs. SNR for 600 Hz for the coherent Bartlett-CLEAN processor and the GS-MAP processor.

An explanation for the poor performance of the coherent Bartlett-CLEAN processor at this frequency can be found in Figure 3 which shows probability of source localization for the coherent Bartlett-CLEAN and MAP processors (also shown in Figure 2) and the probability of correct localization for the coherent Bartlett-CLEAN processor that employs

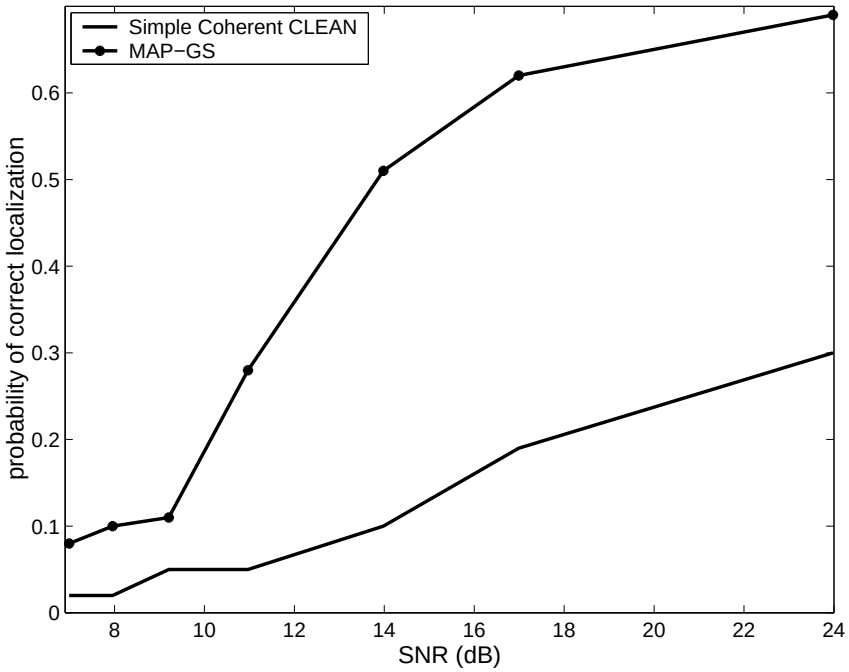


Figure 2: Probability of correct localization vs. SVR for 200 Hz for the coherent Bartlett-CLEAN processor and the GS-MAP processor.

as $\hat{\alpha}_{str}$ the true value of $\alpha_{str}$ (it does not assumes $r_{s,str}$ and $z_{s,str}$ to be known, though, and estimates them by maximizing the ambiguity surface of Equation 1). The latter processor is not realistic because information on $\alpha_{str}$ is not typically available but offers an upper performance bound for the coherent Bartlett-CLEAN processor. For high SNRs, this ideal processor outperforms both the MAP and the realistic coherent Bartlett processor. As the SNR decreases, the MAP processor becomes slightly better than the "artificial" processor. The simple coherent processor always lags behind substantially. Figure 3 illustrates that the cause of the poor performance of the simple coherent Bartlett-CLEAN processor lies in the estimation of $\alpha_{str}$ which is necessary before Equation 8 is used.

Figure 4 demonstrates why the MAP processor does not suffer greatly from the same problem. The figure shows the posterior probability distribution of the complex amplitude of the strong source as obtained from the MAP processor. There is significant probability

concentrated at a phase of 0.5 radians (true value of the phase of that source). There is more uncertainty regarding the source amplitude; we see that the probability distribution exhibits high values for amplitudes roughly between 7 and 24 (the true amplitude is 20). The plot also indicates the point estimate of $\alpha_{str}$ as obtained from the coherent Bartlett-CLEAN processor, which is far away from the true amplitude and phase of the source (it coincides with a secondary mode of the probability distribution). The coherent Bartlett-CLEAN estimator fails to estimate the weak source location using that point estimate. The MAP processor, integrating over the probability distribution of the strong source complex amplitude, correctly identifies the weak source.

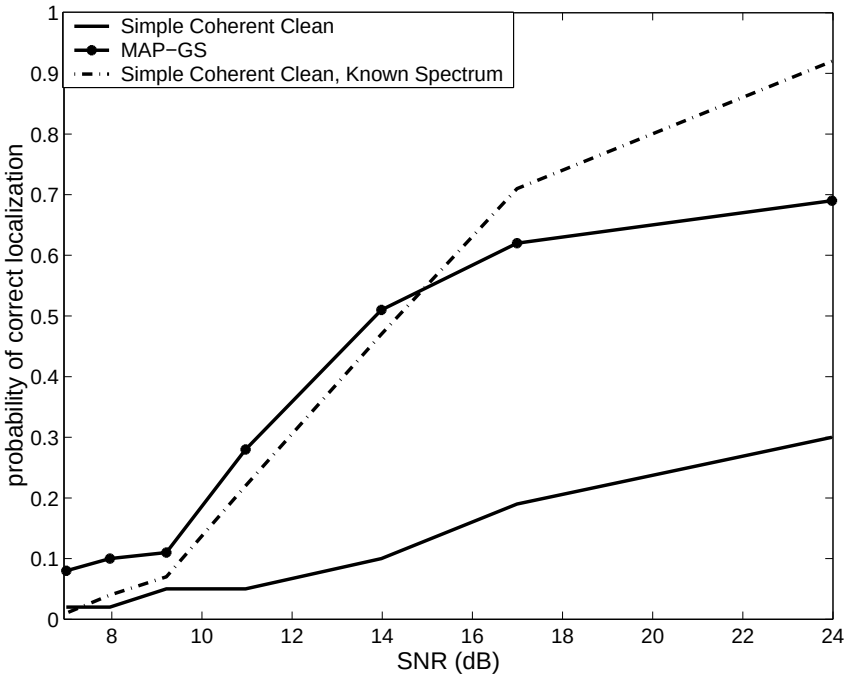


Figure 3: Probability of correct localization vs. SVR for 200 Hz for the coherent Bartlett-CLEAN processor, the GS-MAP processor, and a coherent Bartlett-CLEAN processor that knows exactly the complex amplitude of the strong source.

More simulations were run with data at frequencies between 200 and 600 Hz. It was observed that for these frequencies the two processors had similar performance. With frequencies at and below 200 Hz, there is a significant advantage in using the proposed Gibbs

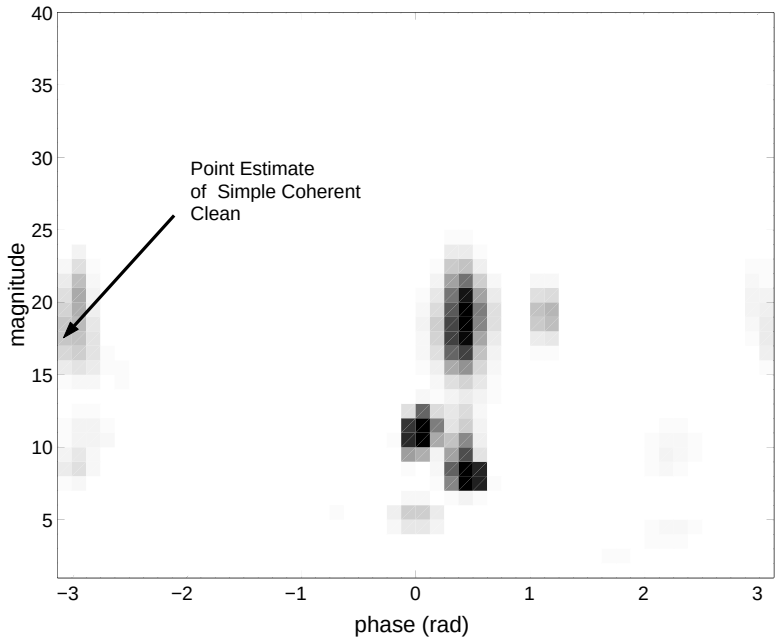


Figure 4: Posterior probability distribution of $\alpha_{str}$, the complex amplitude of the strong source.

Sampling-coherent processor. Figure 5 shows probability of correct localization as obtained from the new processor for the two sources operating at 100 Hz. Although these probabilities are not particularly high, the processor performs better than the simple coherent processor (not shown here) which fails to successfully localize both sources in every single case.

Observing more closely the Gibbs Sampling - MAP coherent cancellation results, we observed that, although even in high SNRs the processor failed in several cases to estimate the two source locations correctly, the approach was quite successful in depth estimation. Figure 6 shows probability of correct depth estimation for both the simple and the proposed processor. The simple coherent processor has a probability of correct depth estimation between 0.33 and 0.45 for all SNRs with an arbitrary pattern of variations. The proposed processor has a probability of correct depth estimation that increases as SNR increases (as expected) and that reaches 0.88 for an SNR of 24 dB. The ability to identify correctly source depth in an environment with interference present is significant, because it answers

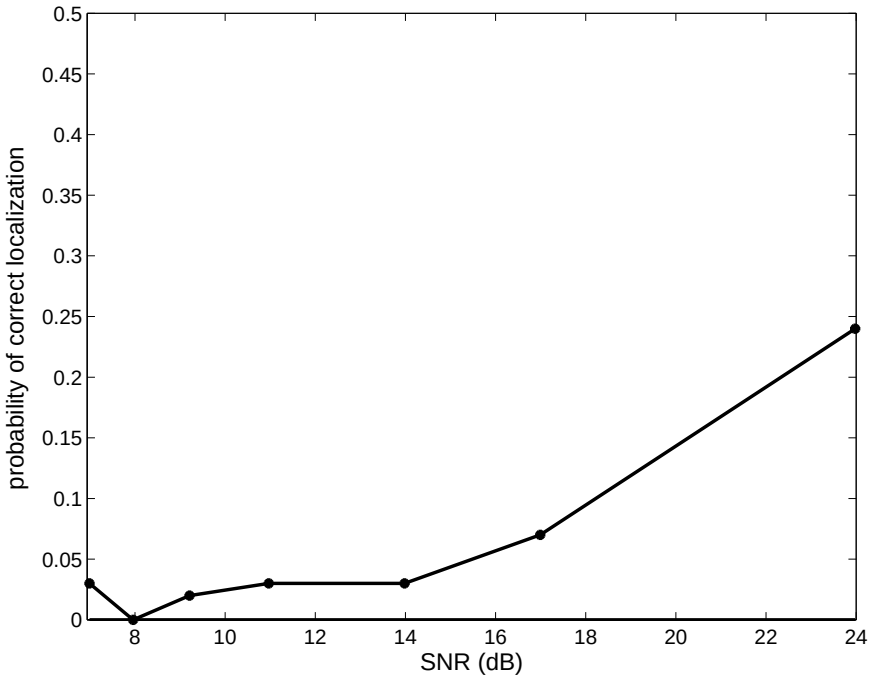


Figure 5: Probability of correct localization vs. SNR for 100 Hz for the the GS-MAP processor.

the question of whether a sensed source is submerged or whether it is located at the surface of the water column.

A coherent multiple source localization approach based on MFP was also proposed in [6]. There, the received signal was modeled as follows:

$$\mathbf{X} = \sum_{i=1}^{M} b_i \mathbf{G}_i(r_i, z_{s,i}) / ||\mathbf{G}_i(r_i, z_{s,i})|| + \mathbf{W}, \tag{15}$$

where $\mathbf{G}$ is a Green's function vector calculated at the $L$ receiving phones and $\mathbf{W}$ is an $L$-dimensional complex, zero-mean noise vector. The model of Equation 15 combines contributions from $M$ sources without involving source levels, which are actually estimated by our method. Coefficients $b_i$ represent received levels: $|b_i|$ is the strength of the contribution of the i$th$ source at the receiving array. As mentioned in [6], source levels were avoided in the modeling in order to circumvent correlations between them and source ranges which might potentially complicate the estimation process. Using the model of Equation 15 and

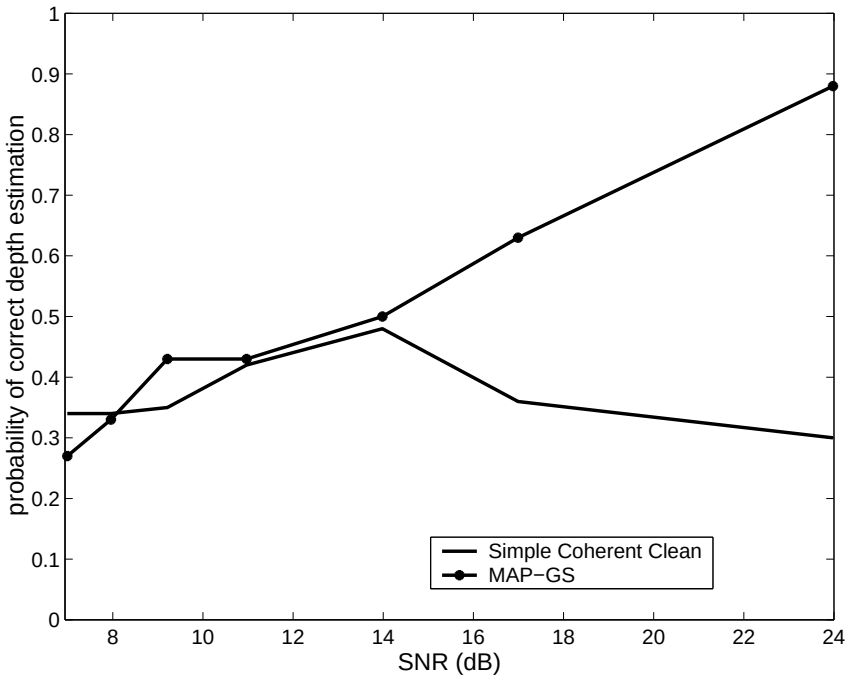


Figure 6: Probability of correct depth estimation vs. SNR for 100 Hz for the coherent Bartlett-CLEAN processor and the GS-MAP processor.

simulated annealing, a search was performed in [6] for the number of sources, their location, and environmental parameters.

To compare our processor to that of [6], we performed source localization of two sources using the model of Equation 15 and estimating posterior distribution $p(r_1, z_{s1}, r_2, z_{s2}, b_1, b_2, \sigma^2|\mathbf{X})$) using Gibbs Sampling. In some cases the results of the process relying on Equation 15 were practically identical to the results of the processor developed here (which uses the model of Equation 9). In other cases, however, after the strong source was identified, the sampling process was "trapped" in this source's neighboring region; as a result, the weak source was not identified and a second source ("shadow" of the actual strong source) was falsely found. Equation 15 removes the effect of two very different source amplitudes from the data; this "smoothing" might account for the difficulty of the processor relying on Equation 15 in identifying both sources. The problem can be remedied by applying restrictions prohibiting the

Gibbs Sampler from searching for the weak source in the vicinity of the strong source. Such restrictions are not necessary for the processor proposed in this work.

# V Unknown number of sources

In the preceding section, the number of sources was assumed known and set equal to two. In practice there is no such precise information on the number of sources. In this section, the assumption of a known source count is relaxed; along with complex source amplitudes, locations, and noise variance, the number of sources is estimated as well.

According to the analysis presented in this paper, the joint probability distribution we have so far estimated with Gibbs Sampling is in reality a conditional distribution, conditioning being on the number of sources $M$: $p(\alpha_1, \ldots, \alpha_M, r_1, z_{s1}, \ldots, r_M, z_{sM}, \sigma^2 | \mathbf{X}, M)$. Following the Bayesian paradigm, a prior distribution can be specified for $M$, and, in like manner with the other parameters, a posterior distribution can be estimated from which we can infer the number of sources present.

In the absence of specific information on $M$, we select a uniform prior over a range believed to be realistic:

$$p(M) = \frac{1}{M_2 - M_1 + 1}, \quad M_1 \leq M \leq M_2, \tag{16}$$

where $M_1$ and $M_2$ are lower and upper bounds for the expected number of sources.

Having already calculated the joint posterior probability distribution of all unknowns, we then compute the marginal posterior distribution $p(M|\mathbf{X})$, where

$$p(M|\mathbf{X}) = \int_{\sigma^2} \int_{\alpha_M} \cdots \int_{\alpha_1} \int_{r_M} \int_{z_{sM}} \cdots \int_{r_1} \int_{z_{s1}} p(\alpha_1, \ldots, \alpha_M, r_1, z_{s1}, \ldots, r_M, z_{sM}, \sigma^2 | M, \mathbf{X}) p(M) \, d\alpha_1 \ldots d\alpha_M \, dr_1 \, dz_{s1} \ldots dr_M \, dz_{sM} \, d\sigma^2 \tag{17}$$

Maximizing Equation 17 yields a MAP estimate of $M$.

One hundred noisy data realizations were generated to test the estimation of the number of sources; the SNR was 14 dB and the frequency was 200 Hz. Two sources were present as in the previous section. Using prior knowledge, it was assumed that $M$ could vary between 1 and 4. The estimated marginal posterior distributions of $M$ for all realizations are exhibited in Figure 7. It is evident that most distributions are maximized for $M = 2$, the true number of sources. Specifically, 99 out of 100 times the maximum occurs for $M = 2$; for one realization, the posterior distribution is maximized for $M = 1$.

In addition to the point estimate $\hat{M} = 2$, our approach also provides information on the uncertainty in the estimation of the number of sources. Variance of $M$ and other moments can be readily calculated from Equation 17. From the distribution of Figure 7, we can see that there is a very small probability of three or four sources being present. It appears that the number of sources is probably two, with one source being the next best choice.

As expected, results deteriorate as the noise increases. Figure 8 shows the marginal posterior distributions of $M$ for all realizations for an SNR of 11 dB. A MAP estimate of 1 is obtained for 50% of the realizations. For the remaining 50%, an estimate $\hat{M} = 2$ is obtained, representing the true number of sources.

Figure 9 shows the posterior distribution of $M$ for a *single* data realization for each of the two considered SNRs. The distribution of $M$ for the lower SNR (Figure 9(b)) exhibits higher variability than the distribution for the higher SNR (Figure 9(a)) with the probability divided between values 2 and 1 for $M$ because of the increased noise level.

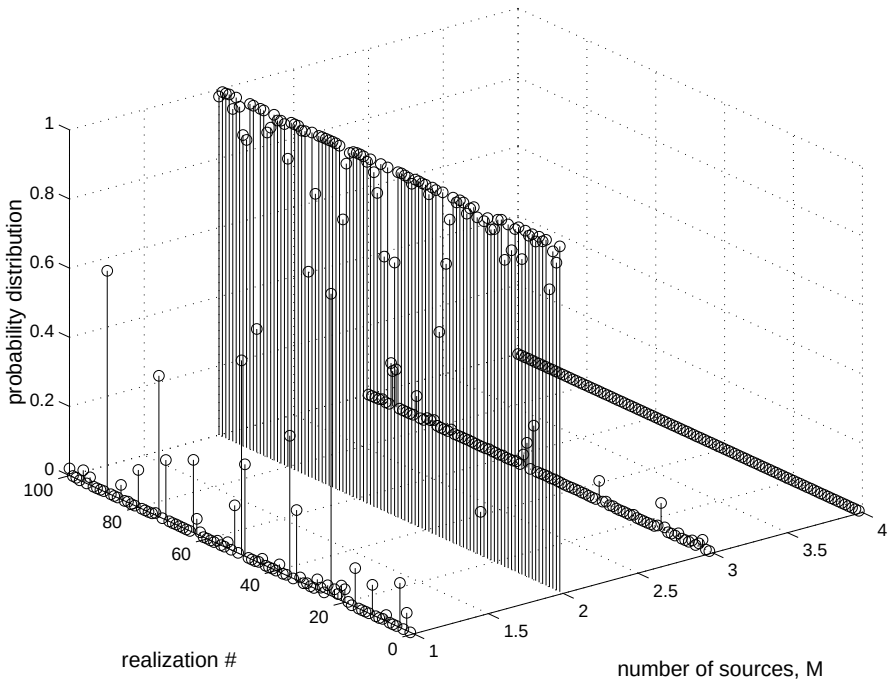


Figure 7: Posterior distribution of $M$ vs. $M$ and realization number: SNR is 14 dB.

# VI Conclusions

A Maximum a Posteriori matched-field estimation approach was developed for localization of multiple sources. The method, optimized with Gibbs Sampling, provides estimates of the number of sources, their locations, and noise variance. The method is, in essence, a deconvolution approach that can remove strong interfering source contributions from the received field for the identification of weaker sources of interest. The new approach was evaluated against interference cancellation methods for multiple source localization previously discussed in the matched-field literature and was found superior for frequencies around and below 200 Hz. The superiority of the method is attributed to integrating over uncertainty instead of relying on point estimates as other methods do. Unlike previously developed methods, our approach also offers posterior probability distributions of the parameters of interest demonstrating the uncertainty present in the estimation problem. With the marginal

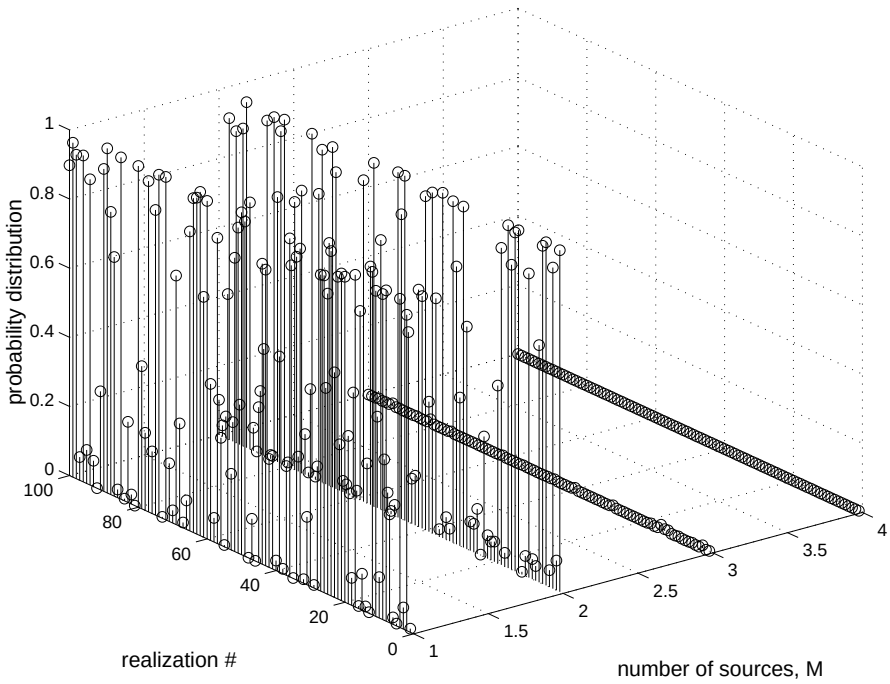


Figure 8: Posterior distribution of $M$ vs. $M$ and realization number: SNR is 11 dB.

conditional distributions of source levels and phases readily available, the approach can also be employed towards source signature estimation. The method as presented here deals with a perfectly known environment. This assumption can be relaxed, and estimates of environmental parameters can be further obtained as in [16].

# VII ACKNOWLEDGMENTS

This work was supported by the Office of Naval Research through grant numbers N00014-97-1-0600 and N00014-05-1-0262. The author is grateful to the NSF DMS-MRI program for computing support.

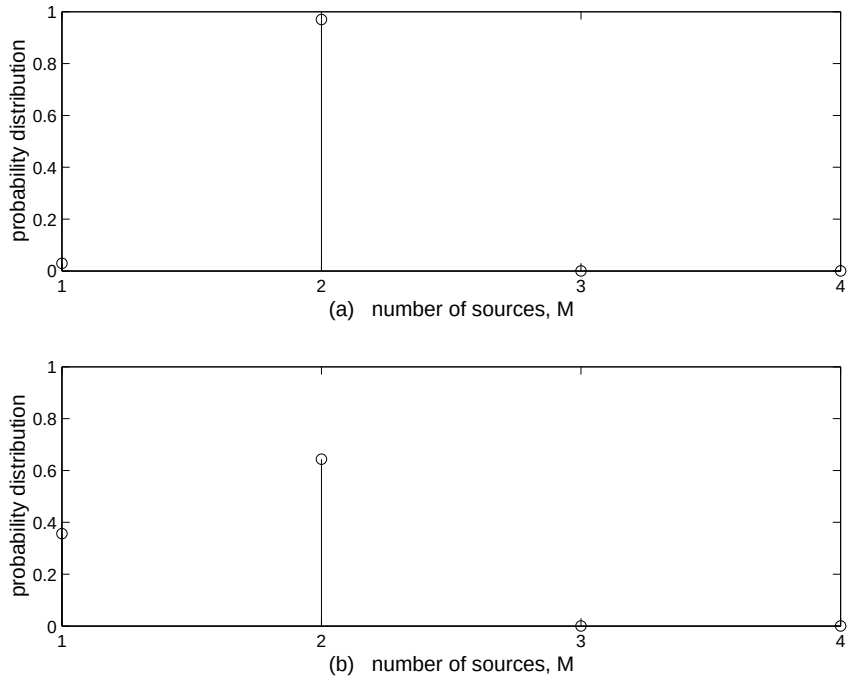


Figure 9: Posterior distribution of $M$ vs. $M$ for a single data realization: SNR is (a) 14 dB and (b) 11 dB.

# References

[1] A. Tolstoy, *Matched Field Processing for Underwater Acoustics*. Singapore: World Scientific, 1993.

[2] A. Baggeroer, W. Kuperman, and P. N. Michalevsky, "An overview of matched field processing in ocean acoustics," *IEEE Journal of Oceanic Engineering*, vol. 18, no. 4, pp. 401–424, 1993.

[3] J. Ozard, "Matched field processing in shallow water for range, depth, and bearing determination: Results of experiment and simulation," *J. Acoust. Soc. Am.*, vol. 86, no. 2, pp. 744–753, 1989.

[4] A. N. Mirkin and L. H. Sibul, "Maximum likelihood estimation of the locations of multiple sources in an acoustic waveguide," *J. Acoust. Soc. Am.*, vol. 95, pp. 877–888,

1994.

[5] M. D. Collins, L. T. Fialkowski, W. A. Kuperman, and J. S. Perkins, "The multi-valued Bartlett procesor and source tracking," *J. Acoust. Soc. Am.*, vol. 97, pp. 235–241, 1995.

[6] M. V. Greening, P. Zakarauskas, and S. E. Dosso, "Matched-field localization for multiple sources in an uncertain environment, with application to Arctic ambient noise," *J. Acoust. Soc. Am.*, pp. 3525–3538, 1997.

[7] L. Zurk, N. Lee, and J. Ward, "Source motion mitigation for adaptive matched field processing," *J. Acoust. Soc. Am.*, vol. 113, no. 5, pp. 2719–2731, 2003.

[8] J. Hőgbom, "Aperture syntesis with a non-regular distribution of interferometer baselines," *Astron. Astrophys. Suppl.*, vol. 15, pp. 417–426, 1974.

[9] U. J. Schwarz, "Mathematical-statistical description of the iterative beam removing technique (method CLEAN," *Astron. Astrophys.*, vol. 65, pp. 345–356, 1978.

[10] Z.-H. Michalopoulou, "The effect of source amplitude and phase on matched field source localization," *J. Acoust. Soc. Am.*, pp. EL21–EL26, 2006.

[11] A. Richardson and L. Nolte, "A posteriori probability source localization in an uncertain sound speed, deep ocean environment," *J. Acoust. Soc. Am.*, vol. 89 (5), pp. 2280–2284, 1991.

[12] S. Geman and D. Geman, "Stochastic relaxation, Gibbs distributions, and the Bayesian restoration of images," *IEEE Transactions on Pattern Analysis and Machine Intelligence*, vol. PAMI-6, pp. 721–741, November 1984.

[13] A. E. Gelfand and A. F. Smith, "Sampling–based approaches to calculating marginal densities," *Journal of the American Statistical Association*, vol. 85, pp. 398–409, November 1990.

[14] J. Besag and P. Green, "Spatial statistics and Bayesian computation," *Journal of the Royal Statistical Society*, vol. 55, no. 1, pp. 25–37, 1993.

[15] W. R. Gilks, S. Richardson, and D. J. Spiegelhalter, *Markov Chain Monte Carlo in Practice*. Chapman and Hall, CRC, first ed., 1996.

[16] S. Dosso, "Quantifying uncertainty in matched field inversion. I A fast Gibbs sampler approach.," *J. Acoust. Soc. Am.*, vol. 111, no. 1, pp. 129–142, 2002.

[17] L. Devroye, *Non–Uniform Random Variate Generation*. Springer Verlag, 1986.

[18] Z.-H. Michalopoulou and M. Picarelli, "Gibbs sampling for time delay and amplitude estimation in underwater acoustics," *J. Acoust. Soc. Am.*, vol. 117, pp. 799–808, February 2005.

[19] M. A. Tanner, *Lecture Notes in Statistics: Tools for Statistical Inference (Observed Data and Data Augmentation Methods)*, vol. 67. Springer Verlag, second ed., 1992.